Atomic Interferometer Based on Adiabatic Population Transfer

Martin Weitz, Brenton C. Young, and Steven Chu
Department of Physics, Stanford University, Stanford, California 94305
(Received 2 June 1994)

We demonstrate an atomic interferometer based on the transfer of population between two ground states via adiabatic following using a nonabsorbing "dark" superposition state. This type of interferometer promises to be useful for precise measurement of the photon recoil energy and also for large area atomic interferometers since it allows transfer of a large number of photon recoil momenta to the atoms with high efficiency. In preliminary experiments, we have obtained a *coherent* transfer efficiency of 95% with transfer of photon momenta and 98.4% with no transfer of momenta. Over 140 photon momenta have been transferred coherently to the atoms.

PACS numbers: 42.50.Vk, 03.75.Dg, 07.60.Ly, 35.80.+s

Several groups have recently shown that laser light can coherently split and recombine atoms [1]. Atom interferometers have been used to measure the acceleration due to gravity [2] with a resolution of 3 parts in 10^8 and 1 part in 10^7 for $\hbar/m_{\text{atom}}$ [3]. In the measurement of $\hbar/m_{\text{atom}}$, we transferred typically ± 32 photon momenta in order to increase the sensitivity of the measurement. The sensitivity of atom interferometers can be increased if improved methods of coherently changing the momentum of the atom are developed. Our previous experiments used beam splitters and mirrors based on stimulated Raman transitions and achieved a transfer efficiency of 85% per pair of photons.

In this Letter, we examine population transfer based on adiabatic passage. This technique was first introduced in nuclear magnetic studies [4] before being carried over into the optical domain [5]. Population transfer by adiabatic passage using delayed laser pulses was first observed by Gaubatz *et al.* [6] in molecular systems, and Marte, Zoller, and Hall [7] proposed the use of this method for atomic beam splitters. Coherent transfer of $6\hbar k$ momentum using adiabatic following has recently been demonstrated by Lawall and Prentiss [8], and $8\hbar k$ was achieved in the work of Goldner *et al.* [9].

We report the coherent transfer of 140 photon momenta to cesium atoms with an efficiency of 95% per exchanged photon pair. We have also constructed the first atom interferometer based on adiabatic population transfer. In this work, we used a magnetic field insensitive transition, which is essential for precision interferometry [2,3]. The adiabatic transfer, done with two counterpropagating laser beams in a σ^+-σ^+ polarization configuration, was between the two cesium hyperfine ground states $6S_{1/2}$, $F = 3$, $m_F = 0$ and $6S_{1/2}$, $F = 4$, $m_F = 0$ via the excited state $6P_{1/2}$, $F' = 3$ or 4, $m_F = 1$. Since both beams have the same helicity, atoms that are not transferred adiabatically will be predominantly optically pumped into $F = 4$, $m_F = +4$ and $F = 3$, $m_F = +3$ states. Thus, the fraction of atoms that are coherently transferred can be measured and the loss of interferometer contrast through nonadiabatic transfers is lessened. In the work of Goldner *et al.* [9] using the cesium D_2 line, off-resonant excitation to other excited states limited the observed efficiency to ~80% per exchanged photon pair. The $6P_{1/2}$ state has a 5.8 times larger excited state hyperfine splitting (1.17 GHz) than the $6P_{3/2}$ state so that the off-resonant excitation using the D_1 line is significantly lower [10]. Also, by shaping the excitation pulses, we were able to improve the transfer efficiency.

Figure 1(a) shows a simplified level scheme for adiabatic transfer, where optical beams of frequencies ω_1 and ω_2 and wave vectors $\mathbf{k}_1$ and $\mathbf{k}_2$ connect two ground states $|1\rangle$ and $|3\rangle$ via an excited state $|2\rangle$. With detuning $\delta = 0$, for any Rabi frequencies $\Omega_1 e^{i\phi_1}$ at ω_1 and $\Omega_2 e^{i\phi_2}$ at ω_2, one of the new eigenstates in the interaction picture (where the atomic oscillation frequencies ω_{12}^A and ω_{23}^A are factored out of the Hamiltonian) is a coherent superposition of the ground states for which the amplitudes for absorption into the excited state cancel [11]. This noncoupled or "dark" state, with eigenvalue zero (i.e., no ac Stark shift), is given by

$$|\nu_D(t), \mathbf{p}\rangle = \cos\theta(t) e^{i\phi_1} |1, \mathbf{p}\rangle - \sin\theta(t) e^{i\phi_2} |3, \mathbf{p} + \hbar\mathbf{k}_1 - \hbar\mathbf{k}_2\rangle, \quad (1)$$

where $\tan\theta(t) = \Omega_1(t)/\Omega_2(t)$. By slowly changing the light intensities with pulse shapes as shown in Fig. 1(b), population can be adiabatically transferred from $|1, \mathbf{p}\rangle$ to $|3, \mathbf{p} + \hbar\mathbf{k}_1 - \hbar\mathbf{k}_2\rangle$ while remaining in the dark state. For counterpropagating laser beams, two photon momenta

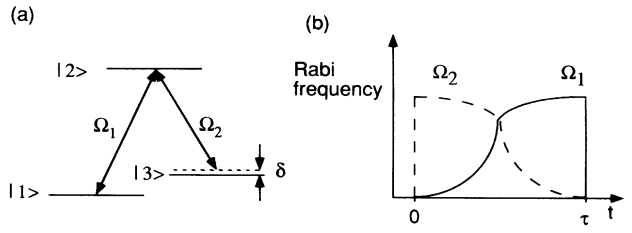

FIG. 1. (a) Level scheme and (b) pulse sequence for complete population transfer for adiabatic following based on delayed laser pulses. The condition for adiabatic following is $\Omega_{\max}\tau \gg 1$.

0031-9007/94/73(19)/2563(4)$06.00

are transferred to the atoms. When the directions of both laser beams are reversed after each transfer, multiple successive interactions give a large momentum transfer.

Adiabatic transfer has some experimental advantages. It is experimentally robust since it is not very sensitive to changes in parameters such as laser power. Also, we have shown that adiabatic transfer in a pure three level system performed with light on resonance does not introduce any ac Stark shift *even when the transfer is not 100% adiabatic* [12]. This fact may have applications in optical frequency standards since one of the major drawbacks of using a two-photon clock transition is the induced ac Stark shift.

The adiabatic transfer method can also be used to construct the necessary atom "beam splitters" for an interferometer as shown in Fig. 2. This interferometer has the four $\pi/2$ geometry first studied by Bordé [13]. A coherent superposition of two states of different momenta is created by turning the intensity of both beams to zero in the middle of a transfer pulse [7] as in pulse A of Fig. 2. If the light is turned off adiabatically with $\Omega_1 = \Omega_2$, the state immediately after pulse A contains $|1,\mathbf{p}\rangle$ and $|3,\mathbf{p} + \hbar\mathbf{k}_1 - \hbar\mathbf{k}_2\rangle$ with equal amplitudes. In pulse B, both Ω_1 and Ω_2 are increased simultaneously. In general, the atom will be found in a superposition of the coupled and noncoupled ground states. As pulse B evolves, the part of the atom in the equal superposition dark state will be adiabatically transferred to the new dark state, $|1,\mathbf{p}\rangle$. Any part of the atom that projects onto the coupled state undergoes spontaneous emission and falls into a number of m_F states, most of which will not be detected. The dotted lines symbolize the loss of atoms out of the dark state. Pulse C takes the part of the atom in the dark state $|1,\mathbf{p}\rangle$ immediately before pulse C and creates another superposition dark state. Finally, pulse D is used to spatially recombine the atom and complete the interferometer.

The interference signal is calculated in a straightforward manner. Assume for the sake of simplicity that the dark state at the end of pulse A at time $t = 0$ is $(1/\sqrt{2})\{|1,\mathbf{p}\rangle - |3,\mathbf{p} + \hbar\mathbf{k}_1 - \hbar\mathbf{k}_2\rangle\}$. If the driving laser fields are in exact resonance with the dark state precession frequency, the entire atom will be transferred by pulse B into dark state $|1,\mathbf{p}\rangle$. In general, there is an initial spread in atomic momenta $f(p_z)$ along the direction parallel to $\mathbf{k}_1$ and $\mathbf{k}_2$, so the laser frequency will not be in exact resonance. The two-photon detuning for the first two

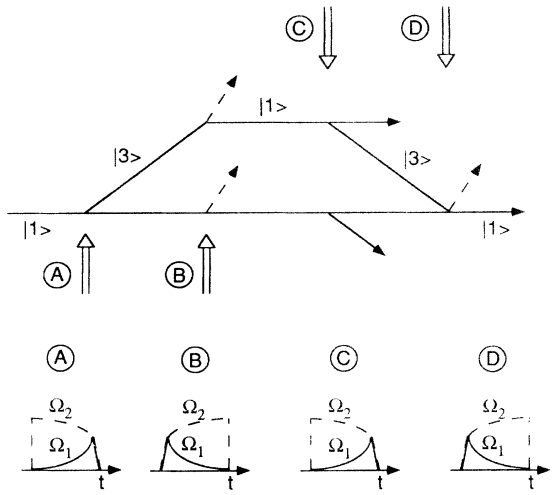

FIG. 2. Scheme and pulse sequence for an atomic interferometer using adiabatic following. The double arrows show the propagation axis of the light with frequency ω_1 (Rabi frequency Ω_1); light with frequency ω_2 (Rabi frequency Ω_2) is directed oppositely. The dashed lines show loss of atoms due to spontaneous emission.

pulses (for $\mathbf{k}_1 = k_1\mathbf{e}_z$, $\mathbf{k}_2 = -k_2\mathbf{e}_z$, $k \sim k_1 \sim k_2$) is $\delta = \Delta\omega - 2kp_z/m - \omega_r$, where $\Delta\omega \equiv \omega_1 - \omega_2 - \omega_{\mathrm{HFS}} - (\mathbf{k}_1 - \mathbf{k}_2)\cdot\mathbf{g}t$, ω_{HFS} denotes the ground state splitting, $\omega_r = 2\hbar k^2/m$ is the recoil energy of the two-photon transition, and the final term in $\Delta\omega$ accounts for the Doppler shift due to gravity during a free fall of time t. At the time $t = T$ of pulse B, the portion of the state in phase with the dark state is the projection

$$\frac{1}{2}\left(\langle 1,\mathbf{p}| - e^{+i\delta T}\langle 3,\mathbf{p} + \hbar\mathbf{k}_1 - \hbar\mathbf{k}_2|\right) \cdot \left(|1,\mathbf{p}\rangle - |3,\mathbf{p} + \hbar\mathbf{k}_1 - \hbar\mathbf{k}_2\rangle\right) = \frac{1}{2}\left(1 + e^{+i\delta T}\right). \tag{2}$$

After summing over all the momentum states, the portion of the atomic wave function after the second pulse is given by

$$|\Psi(t)\rangle = \int f(p_z)\,|\nu_D(t), p_z\rangle \frac{1 + e^{+i(\Delta\omega - 2kp_z/m - \omega_r)T}}{2}\,dp_z\,. \tag{3}$$

For pulses C and D, the directions of the two beams are reversed, giving a two-photon detuning of $\delta = \Delta\omega + 2kp_z - \omega_r$, and another factor as in Eq. (2) is introduced. After the final pulse, the part of the wave function in the dark state is

$$|\Psi(t)\rangle = \int f(p_z)\,|\nu_D(t), p_z\rangle \frac{\left[1 + e^{+i2(\Delta\omega - \omega_r)T} + 2e^{+i(\Delta\omega - \omega_r)T}\cos 2kp_zT/m\right]}{4}\,dp_z\,, \tag{4}$$

where the difference frequency is assumed to compensate for the gravitational shift so that $\Delta\omega$ is equal for all pulses. The second term in the brackets gives the fringes, while the last term averages to zero after integration over a broad velocity distribution. At the interference maxima the dark state is maximally populated, and at the interference minima the coupled state is predominately populated and spontaneously decays.

Our experimental setup shown in Fig. 3 is similar to our previously described atomic fountain apparatus [2,3,14]. A cesium atomic beam, slowed by a chirped laser beam, loaded a magneto-optic trap [15]. The light necessary for cooling and trapping was generated from a Ti:sapphire laser operating at the cesium D_2 transition $6S_{1/2}-6P_{3/2}$. In 0.4 s about 10^9 atoms were loaded, after which the trapping magnetic field was shut off and the atoms were further cooled to 4 μK in polarization-gradient optical molasses [16]. The atoms were then launched in a vertical ballistic trajectory by acousto-optically shifting the molasses beams' frequencies to a moving molasses [17] traveling upwards at 2.3 m/s. The molasses beams were then blocked with a mechanical shutter. On their way up, the atoms were optically pumped into $F = 4$, $m_F = 0$ and entered a magnetically shielded region with a homogeneous 100 mG magnetic bias field oriented parallel to the Raman beams. While the atoms were in the shielded region, a series of adiabatic pulses of the Raman beams was applied. The pulse sequence was designed to leave the coherently transferred atoms in $F = 3$, $m_F = 0$. As the atoms dropped back down, a laser beam tuned to $6S_{1/2}, F = 4-6P_{3/2}, F' = 5$ pushed away residual $F = 4$ population. The $F = 3$, $m_F = 0$ population was measured by first transferring the population to $F = 4$, $m_F = 0$ with a microwave π pulse. Then, after the atoms had fallen back into the probe beam region, light tuned to $6S_{1/2}, F = 4-6P_{3/2}$, $F' = 5$ was pulsed on and the subsequent fluorescence was measured.

The two Raman beams were generated from a second Ti:sapphire laser locked to the D_1 $F = 4-F' = 3$ or 4 transition at 894 nm. The second Raman frequency component at $F = 3-F'$ was generated by directing part of the beam through a 9.2 GHz electro-optic modulator (EOM) and then through a cavity locked to the upper sideband. The cavity filtered out all optical frequencies by 35 dB except for the desired sideband. Two 40 MHz acousto-optic modulators (AOM's 1 and 2) were used to generate the pulse shapes for adiabatic following, as shown in Figs. 1(b) and 2.

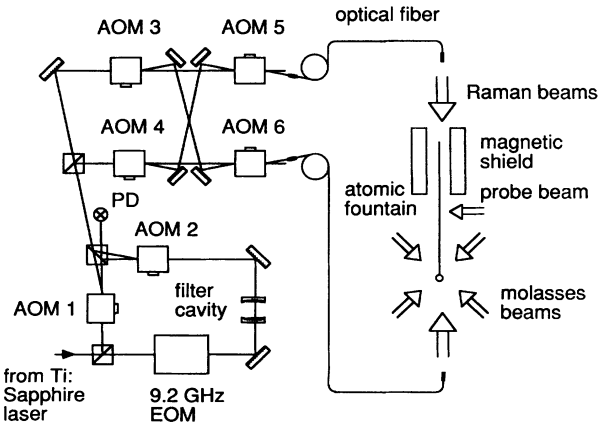

FIG. 3. Experimental setup used for an atomic interferometer based on delayed laser pulses. The optics used to generate the beams for the atomic fountain are not shown and we have omitted the slowing, clearing, and hyperfine pumping beams.

The undeflected fraction of both acousto-optic modulators were mixed on a fast photodiode and the beat frequency was phase locked to an rf source by controlling the electro-optic modulator drive frequency. This difference frequency was adjusted between each pulse to account for the gravitational acceleration of the atoms. In order to obtain large momentum transfers, the directions of the Raman beams were switched after each transfer with a set of four acousto-optic modulators. When AOM's 3 and 4 were on while AOM's 5 and 6 were off, $F = 4$ light came from below and $F = 3$ light from above. The directions were reversed when AOM's 5 and 6 were on while AOM's 3 and 4 were off. The beams were then coupled into single mode optical fibers and expanded to a 2 cm Gaussian diameter with 6 mW/beam.

For efficient transfer, the Doppler width of the atoms has to be significantly smaller than the frequency width of the resonance. If an atom is partially out of resonance with the laser fields, there is nonzero amplitude for excitation out of the dark state. For the first $F = 4$, $m_F = 0$ to $F = 3$, $m_F = 0$ transfer pulse, we used a low intensity, 800 μs pulse to select a 17 kHz Doppler width velocity slice (FWHM) from the initial molasses velocity distribution of 90 kHz.

We studied the transfer efficiency by applying, after velocity selection, a variable number of complete population transfer pulses and noting the final $m_F = 0$ population. We measured the momentum transfer (up to 70 pulses, corresponding to 140 photon momenta) from a change in the arrival time of the atoms in the probe region and from the Doppler shift of the two-photon resonance of the transfer pulses. The efficiency is sensitive to the purity of the Raman beam polarizations; if the two beams have different polarizations the dark state will not be a pure $m_F = 0$ state. For Doppler-free transitions, same polarizations can be ensured with great precision because both beams can pass through the same optics, and we were able to obtain an efficiency of 98.6% per transfer pulse. Back reflections from the vacuum windows can also limit the transfer efficiency in the Doppler-sensitive case since the moving atoms would be exposed to light with incorrect Raman difference frequencies.

In the Doppler-sensitive mode, we obtained an efficiency of 95.7%, limited by $\sim 10^{-3}$ polarization imperfections of the quarter wave plates used to generate circularly polarized beams. Of the small fraction of atoms that spontaneously decay during the transfers, some fall back into the $m_F = 0$ dark state. From the known branching ratios, we calculate that the observed efficiencies correspond to coherent transfer efficiencies of 98.4% and 95%, respectively. We calculated a maximum coherent transfer of 98.7%, limited by the excited state off-resonant absorption from the spectator $6P_{1/2}$ hyperfine level [12]. In order to achieve maximum transfer efficiency in the

Doppler-sensitive case, the polarization purity and back reflections must be controlled to roughly 1 part in 10^4.

After obtaining efficient population transfer, we constructed an atomic interferometer using a velocity selection pulse followed by a pulse sequence as shown in Fig. 2 (typical pulse lengths $\tau = 150$ μs). Our experimental results are shown in Fig. 4 for a spacing $T = 250$ μs between both pairs of pulses. The fringes in the final $m_F = 0$ population were recorded as the Raman difference frequency of the final two pulses was varied. The broad envelope in the fringes corresponds to the frequency width of a single pulse. The measured fringe contrast is 29% when using $6P_{1/2}$, $F' = 3$ as the excited state (which is comparable to that observed in the 4 $\pi/2$-pulse interferometer experiment based on detuned Raman pulses of Ref. [3] and 17% with the $F' = 4$ excited state. The expected fringe contrast would be 50% if all atoms that are not transferred adiabatically, and thus spontaneously decay from $6P_{1/2}$, F', $m_F = 1$, would be optically pumped into an outer m_F state. Assuming that half of the atoms that decay into $F = 3$, $m_F = 0$ or $F = 4$, $m_F = 0$ fall into the dark state, the expected fringe contrasts are reduced to 33% ($F' = 3$) and 23% ($F' = 4$). We conjecture that the experimental fringe contrast is less than the theoretically predicted contrast because of imperfect polarization. We also have observed similar fringes for an interferometer with opposite recoil shift in which the atom is in the other internal state between the two pairs of pulses (see Ref. [12] for the pulse sequence).

We have observed good contrast interferometer fringes with a spacing between pulses of up to $T = 1.3$ ms, corresponding to a total interferometer measurement time of ~3.5 ms. For longer spacings the contrast began to wash out because of the frequency jitter on the Raman beams induced by vibrations. By using a vibration isolation system with a feedback circuit, we hope to substantially increase the interferometer drift time [18].

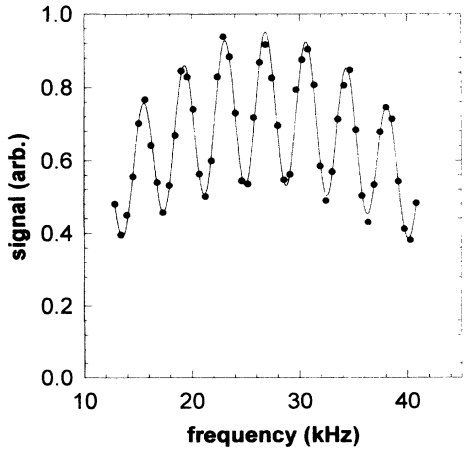

FIG. 4. Interference fringes for an atomic interferometer based on adiabatic following using pulse shapes as shown in Fig. 2. The time between pulses A and B and also C and D was $T = 250$ μs. Pulses B and C were also separated by 250 μs. Each point corresponds to 4 launches at a rate of 0.9 launche/s. The solid line is a fit by a cosine function with a Gaussian envelope.

We plan to use an adiabatic transfer interferometer in our next measurement of $\hbar/m_{\text{atom}}$ [3]. The adiabatic transfer method should allow us to insert more photon recoil momenta than our previous measurement and induce smaller ac Stark shifts. More significantly, we will have two different interferometer methods with different systematics for measuring $\hbar/m_{\text{atom}}$. This method can also be used in large area atom interferometers with extremely high sensitivity to inertial effects.

We acknowledge helpful discussions with Mark Kasevich and Peter Zoller. M. W. acknowledges support from the Deutsche Forschungsgemeinschaft. This work was supported in part by grants from AFOSR and NSF.

[1] See, for example, Appl. Phys. B **54**, 321ff (1992).
[2] M. Kasevich and S. Chu, Phys. Rev. Lett. **67**, 181 (1991).
[3] D. S. Weiss, B. C. Young, and S. Chu, Phys. Rev. Lett. **70**, 2706 (1993); D. S. Weiss, B. C. Young, and S. Chu (to be published).
[4] A. Abragam, *The Principles of Nuclear Magnetism* (Oxford Univ. Press., London, 1961).
[5] D. Grischkowsky, Phys. Rev. Lett. **24**, 866 (1970).
[6] U. Gaubatz, P. Rudecker, M. Becker, S. Schiemann, M. Külz, and K. Bergmann, Chem. Phys. Lett. **149**, 463 (1988).
[7] P. Marte, P. Zoller, and J. L. Hall, Phys. Rev. A **44**, R4118 (1991).
[8] J. Lawall and M. Prentiss, Phys. Rev. Lett. **72**, 993 (1994).
[9] L. S. Goldner, C. Gerz, R. J. C. Spreew, S. L. Rolston, C. I. Westbrook, W. D. Phillips, P. Marte, and P. Zoller, Phys. Rev. Lett. **72**, 997 (1994).
[10] P. Pillet, C. Valentin, R.-L. Yuan, and J. Yu, Phys. Rev. A **48**, 845 (1993).
[11] E. Arimondo and G. Orriols, Lett. Nuovo Cimento **17**, 333 (1976).
[12] M. Weitz, B. C. Young, and S. Chu, Phys. Rev. A **50**, 2438 (1994).
[13] Ch. J. Bordé, Phys. Lett. **A 140**, 10 (1989); F. Riehle, Th. Kisters, A. Witte, J. Helmcke, and Ch. J. Bordé, Phys. Rev. Lett. **67**, 177 (1991).
[14] M. Kasevich, E. Riis, S. Chu, and R. G. DeVoe, Phys. Rev. Lett. **63**, 612 (1989).
[15] E. L. Raab, M. Prentiss, A. Cable, S. Chu, and D. E. Pritchard, Phys. Rev. Lett. **59**, 2631 (1987).
[16] J. Dalibard and C. Cohen-Tannoudji, J. Opt. Soc. Am. B **6**, 2023 (1989); P. J. Ungar, D. S. Weiss, E. Riis, and S. Chu, J. Opt. Soc. Am. B **6**, 2058 (1989).
[17] D. S. Weiss, E. Riis, K. A. Moler, and S. Chu, in *Light Induced Kinetic Effects on Atoms, Ions, and Molecules*, edited by I. Moi, S. Gozzini, C. Gabbanini, E. Arimondo, and F. Strumia (ETS Editrice, Pisa, 1991), p. 35.
[18] A. Peters, J. Hensley, and S. Chu (to be published).